Synthetic Methodology Allowing the Interconversion of Titanium–Oxygen Single Bonds and Double Bonds: The Self-Assembly of Bridging and Terminal Oxotitanium(IV) into Oligomeric and Polymeric Linear Titanoxanes

Federico Franceschi, Emma Gallo, Euro Solari, Carlo Floriani,* Angiola Chiesi-Villa, Corrado Rizzoli, Nazzareno Re, and Antonio Sgamellotti

Abstract: The controlled ionization of the linear [Cl–Ti–O–Ti–Cl] skeleton allowed the generation of the $[Cl–Ti–O=Ti]^+$ dimer, which is nonsymmetrical as a consequence of extended Cl–Ti–O π interactions. The [Ti=O] unit thus formed is a building block for a variety of titanoxane structures. This chemistry has been investigated from a theoretical point of view by ab initio MO analysis of the [Cl–Ti–O–Ti–Cl] and $[Cl–Ti–O=Ti]^+$ fragments. These calculations lead to the conclusion that single ionization generates the [Ti=O] unit, whereas double ionization does not affect the μ-oxo bonding mode in $[Ti–O–Ti]^{2+}$ or $[S–Ti–O–Ti–S]^{2+}$ (where S is a pure σ-donor ligand or solvent). This observation has been confirmed experimentally by ionizing the following model complexes: [(Cl)(acacen)-Ti–O–Ti(acacen)(Cl)] (**3**) (acacen = *N*,*N*′-ethylenebisacetylacetoneiminato dianion) and [(Cl)(salen)Ti–O–Ti(salen)-(Cl)] (**4**) (salen = N,N′-ethylenebissalicylideneiminato dianion), where the linear Cl–Ti–O–Ti–Cl unit is assured by the square-planar bonding mode of the tetradentate Schiff base ligand. The double ionization of **3** with $AgNO_3$ gave the conventional μ-oxo derivative [(acacen)(η^1-ONO_2)Ti–O–Ti(acacen)(η^1-ONO_2)] (**5**). In contrast, the stepwise ionization of **3** and **4** with $NaBPh_4$ in THF led to the non-symmetrical $[Cl–Ti–O=Ti]^+$ intermediates, which are the parent compounds for a variety of linear titanoxanes. The following species containing a Ti=O unit have been isolated from the $NaBPh_4$-assisted ionization of **3**: [(acacen)Ti=O–BPh_3] (**6**) and [(L)(acacen)Ti=O–Ti(acacen)–O-(acacen)Ti–O=Ti(acacen)(L)]$^{2+}$ 2 BPh_4^- (L = THF, **7**; L = none, **8**). The same reaction carried out on **4** led to [(THF)-(salen)Ti=O–Ti(salen)–O–(salen)Ti-(THF)]$^{2+}$ 2BPh_4^- (**9**) and [(L)(salen)-Ti=O–Ti(salen)–O–(salen)Ti–O=Ti-(salen)(L)]$^{2+}$ 2BPh_4^- (L = THF, **10**; L = Py, **11**; L = none, **12**, polymeric form). A scheme is proposed to explain the formation of the species derived from the single ionization of **3** and **4**, where the origin and the binding properties of the [Ti=O] unit play a major role.

Keywords
ab initio calculations · inorganic polymers · mechanistic studies · titanium compounds · titanoxanes

Introduction

In the synthetically intriguing field of titanoxanes[1]—a particularly relevant class of compound that bridges the gap between molecular and solid-state chemistry[2]—we have been searching for general synthetic strategies other than the hydrolysis reaction, which is difficult to control. One of the strategies we developed some years ago was reductive aggregation,[3] which was particularly appropriate in the case of electron-rich aggregates. For the titanium(IV)-based titanoxanes, however, hydrolytic self-assembly, though uncontrolled, is usually the preferred method.[2, 4] Another approach—the one we shall focus on in this paper—involves manipulating the chemistry of the [Ti–O] functionality. This occurs in two forms, namely, bridging [Ti-O-Ti][5] and terminal [Ti=O]. The latter is reactive, though quite rare.[6, 7] The self-assembly of the [Ti–O] unit relies on the interconversion of these two functionalities, and, consequently, on creating building blocks for the aggregation process.

The present report deals with the experimental and theoretical chemistry of the interconversion of these functionalities and how they self-organize into oligomeric and polymeric linear titanoxanes. To this end, we chose the readily accessible [(Cl)(acacen)Ti-O-Ti(acacen)(Cl)][8] and [(Cl)(salen)Ti-O-Ti-(salen)(Cl)][9] complexes (Scheme 1) as model compounds, where the bonding mode of the Schiff base forces the [Cl-Ti-O-Ti-Cl] unit to be linear.

A preliminary consideration of the push–pull synergy[10] in the context of the extended Cl-Ti-O-Ti-Cl π interaction allowed us to enter the area of titanoxanes[4] in a rather unconventional way. A preliminary communication on the subject was recently published.[11]

[*] Prof. Dr. C. Floriani, Dr. E. Gallo, Dr. E. Solari, F. Franceschi
Institut de Chimie Minérale et Analytique
Université de Lausanne, BCH, CH-1015 Lausanne (Switzerland)
Fax: Int. code +(21)692-3905
e-mail: carlo.floriani@icma.unil.ch
Prof. Dr. A. Chiesi-Villa, Dr. C. Rizzoli
Dipartimento di Chimica, Università di Parma
Viale delle Scienze, I-43100 Parma (Italy)
Prof. Dr. A. Sgamellotti, Dr. N. Re
Dipartimento di Chimica, Università di Perugia
Via Elce di Sotto 8, I-06100 Perugia (Italy)

0947-6539/96/0211-1466 $ 15.00+.25/0 Chem. Eur. J. 1996, 2, No. 11

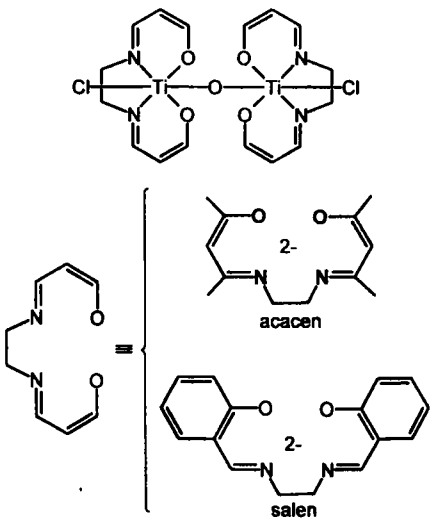

Scheme 1.

Results

a) Synthesis and Structure of Titanoxanes: The starting materials that we considered for the interconversion of the Ti–O functionality and for the transformation into titanoxane aggregates are complexes **3** and **4**. They were obtained in quantitative yield as red crystalline solids by reacting the corresponding titanium(III) derivatives **1**[8] and **2**[9] with dry oxygen (Scheme 2).[8]

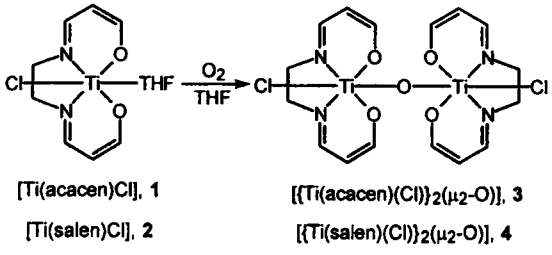

[Ti(acacen)Cl], **1** [{Ti(acacen)(Cl)}2(μ2-O)], **3**

[Ti(salen)Cl], **2** [{Ti(salen)(Cl)}2(μ2-O)], **4**

Scheme 2. Synthesis of starting materials **3** and **4**.

The essential structural features of these starting materials are the linearity of the [Cl-Ti-O-Ti-Cl] skeleton and the rather short Ti–O bond [1.813(1) Å, **3**]. Strong Ti–O stretching vibrations are observed in the IR spectrum at 743 and 765 cm^{-1}, associated with **3** and **4**, respectively. The starting materials **3** and **4** were submitted to the ionization reaction of the Ti–Cl bond, with either $AgNO_3$ or $NaBPh_4$; the former is a much stronger ionizing agent than the latter. The differences in the solubility and in the conformation of the Schiff-base ligand influence the isolation of intermediates and the aggregation mode of the [Ti–O] units.

The reaction of **3** with $AgNO_3$ was carried out in refluxing THF, with the aim of replacing the two axial Cl^- ligands with NO_3^- (Scheme 3). The former is a good σ and π donor, whereas the latter is exclusively a σ donor. The resulting complex **5** was characterized by standard methods. The structure was elucidated by X-ray analysis (Fig. 1, Tables 1 and 2), and the IR spectrum showed the Ti-O-Ti asymmetric stretching frequency at 767 cm^{-1}.

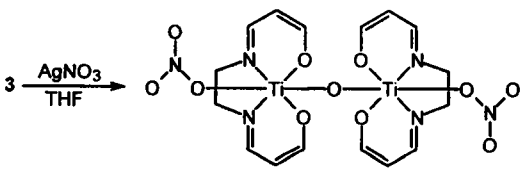

[{Ti(acacen)(η1-ONO2)}2(μ2-O)], **5**

Scheme 3. Replacement of two axial Cl^- ligands with NO_3^- ligands.

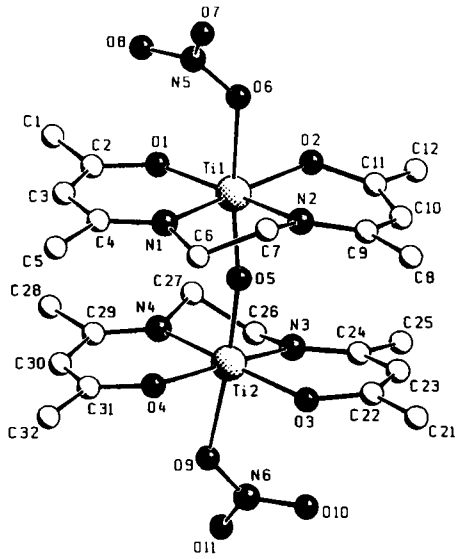

Fig. 1. SCHAKAL drawing of complex **5**.

Table 1. Selected bond lengths (Å) and angles (°) for complex **5**.

Ti1–O5	1.802(4)	Ti2–O5	1.802(4)
Ti1–O1	1.868(4)	Ti2–O3	1.879(4)
Ti1–O2	1.878(4)	Ti2–O4	1.880(4)
Ti1–O6	2.136(5)	Ti2–O9	2.137(5)
Ti1–N1	2.132(5)	Ti2–N3	2.122(5)
Ti1–N2	2.127(5)	Ti2–N4	2.124(5)
Ti1-O5-Ti2	169.7(3)		
N1-Ti1-N2	78.2(2)	N3-Ti2-N4	78.2(2)
O2-Ti1-N2	86.1(2)	O4-Ti2-N4	85.9(2)
O2-Ti1-N1	162.7(2)	O4-Ti2-N3	160.6(2)
O1-Ti1-N2	162.5(2)	O3-Ti2-N4	163.3(2)
O1-Ti1-N1	85.9(2)	O3-Ti2-N3	86.2(2)
O1-Ti1-O2	108.5(2)	O3-Ti2-O4	108.0(2)
O5-Ti1-O6	171.9(2)	O5-Ti2-O9	172.5(2)

The [Ti(acacen)] moiety in **5** has structural parameters very close to those of **3**[8] (Table 1). The N1,N2,O1,O2 core is planar, the Ti1 atom is displaced from it by 0.145(1) Å. The N3,N4,O3,O4 core shows small but significant tetrahedral distortions, Ti2 being displaced by 0.168(1) Å (Table 2). Both titanium atoms are displaced towards the central O5 oxo group. The conformation of the acacen ligand is described by the parameters quoted in Table 2. The O1,C2,C3,C4,N1,Ti1 and O4,C31,C30,C29,N4,Ti2 six-membered rings are nearly planar, while the N2,C9,C10,C11,O2,Ti1 and O3,C22,C23, C24,N3,Ti2 six-membered chelation rings are slightly folded along the N···O lines. These two pairs overlap and are almost parallel with a dihedral angle of 4.6(1) and 7.4(1)°, respectively. The five-membered rings assume a λ conformation for both independent acacen ligands (with respect to the coordinates of Table S2 in Supplementary Material). Since the space group is chiral, the δ,δ conformer is not present in the structure. The two Ti1–O6 [2.136(5) Å] and Ti2–O9 [2.137(5) Å] distances are in the usual range found for terminal nitrate bonds (e.g., 2.086, 2.059,[12] 2.147 Å[13]). The nitrate anions are oriented to form

Table 2. Structural parameters within the Ti(Schiff base) moieties for complexes **5**, **6**, **10**, and **12**.

	5	**6**	**10**	**12**
Dist. from N_2O_2 cores, Å				
O1	0.001(4)	−0.043(4)	−0.004(7)	−0.027(6)
O2	−0.001(4)	0.025(3)	0.004(7)	0.027(6)
N1	−0.002(5)	0.057(5)	0.009(9)	0.052(7)
N2	0.002(5)	−0.057(5)	−0.009(9)	−0.052(7)
Ti1	0.145(1)	0.521(1)	0.302(2)	0.280(2)
O3	0.030(4)		0.025(7)	0.008(6)
O4	−0.035(5)		−0.025(7)	−0.008(6)
N3	−0.044(5)		−0.049(9)	−0.010(6)
N4	0.044(5)		0.049(9)	0.010(6)
Ti2	0.168(1)		0.081(2)	0.118(2)
Folding along/° [a]				
N1···O1	4.0(2)	12.1(2)	14.1(3)	39.5(3)
N2···O2	21.4(2)	27.0(2)	27.2(3)	3.3(3)
N3···O3	13.7(2)		14.9(3)	13.2(3)
N4···O4	5.3(2)		3.3(3)	26.4(3)
Angles between planes, °				
Ti1-N1-O1/Ti1-N2-O2	11.4(2)	42.1(2)	23.5(3)	21.6(3)
Ti2-N3-O3/Ti2-N4-O4	13.7(2)		7.1(3)	9.2(2)
mean O1-C_3-N1/O2-C_3-N2	13.9(2)	5.4(2)	17.6(4)	15.6(3)
mean O3-C_3-N3/O4-C_3-N4	6.0(2)		5.6(3)	5.3(2)
Torsion angles, °				
N1-C-C-N2	−43.0(7)	44.4(7)	−35.8(14)	47.3(8)
N3-C-C-N4	−49.0(7)		43.7(12)	−46.2(7)
Dist. from Ti1-N1-N2 plane, Å [b]				
C8	−0.257(8)	0.557(7)	−0.221(13)	0.249(9)
C9	0.300(7)	−0.018(7)	0.268(14)	−0.402(9)
Dist. from Ti2-N3-N4 plane, Å				
C28	−0.207(7)		0.281(12)	−0.370(9)
C29	0.442(7)		−0.296(12)	0.265(7)

[a] The folding is defined as the dihedral angle between the Ti,N,O and OC_3N planes of a six-membered chelation ring. [b] For complexes **5** and **6**, C8, C9, C28, C29 should be read as C6, C7, C26, C27.

dihedral angles of 58.2(2) and 59.5(2)° with the N_2O_2 cores around Ti1 and Ti2, respectively. The key structural parameters of **5** relating to the Ti-O-Ti fragment [Ti–O, 1.802(4) Å and Ti-O-Ti, 169.7(3)°] are very close to those of **3**, despite the difference in σ- and π-donor properties of NO_3^- and Cl^-.

When a less efficient ionizing agent than $AgNO_3$ was used, such as $NaBPh_4$, the chlorides were replaced in a slow, stepwise process. Thus, we observed a very different result. The reaction of **3** with $NaBPh_4$ was speeded up by refluxing the THF suspension overnight. By making use of their different solubilities in Et_2O, **6** and **7** could be separated from the resulting solid mixture (Scheme 4). The structure of **6** is shown in Figure 2 (the structure of **7** can be found in the Supplementary Material, Figs. S1, S7, S11). Selected bond lengths and angles are given in Table 3. The Ti–O–B bridge is almost linear [Ti–O3–B, 164.6(3)°], the Ti–O3 bond [1.682(3) Å] largely retaining its multiple bond character. The B1–O3 distance is 1.547(7) Å.

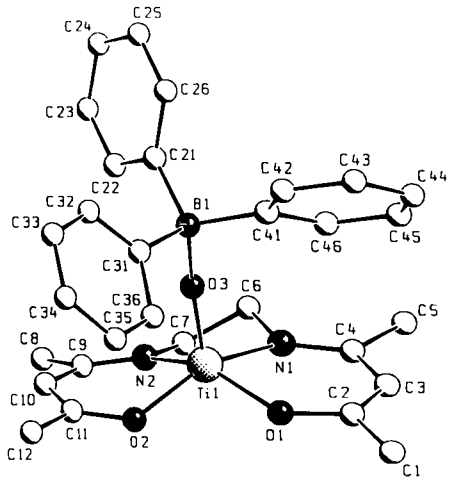

Fig. 2. SCHAKAL drawing of complex **6**.

Table 3. Selected bond lengths (Å) and angles (°) for complex **6**.

Ti1–O3	1.682(3)	Ti1–N2	2.093(5)
B1–O3	1.547(7)	B1–C21	1.630(7)
Ti1–O1	1.877(4)	B1–C31	1.630(8)
Ti1–O2	1.891(3)	B1–C41	1.611(8)
Ti1–N1	2.115(5)		
Ti1-O3-B1	164.6(3)	O1-Ti1-N2	144.6(2)
N1-Ti1-N2	78.3(2)	O1-Ti1-N1	83.6(2)
O2-Ti1-N2	85.0(2)	O1-Ti1-O2	96.8(2)
O2-Ti1-N1	150.5(2)		

The square-pyramidal coordination of titanium is probably due to the labilizing effect of the Ti=O unit on the *trans* ligand. The Ti–O3 bond forms an angle of 2.5(1)° with the perpendicular of the basal N_2O_2 core, from which titanium is displaced by 0.521(1) Å towards the oxo oxygen (Table 2). In square-pyramidal complexes the Ti(acacen) moiety usually assumes an umbrella conformation[8, 14] as a consequence of the folding of the six-membered chelation rings along the N···O lines (Table 2). The five-membered chelation ring has a δ conformation. Since the space group is centrosymmetric, both δ and λ conformers are present in the structure.

Complex **7** has been fully characterized by X-ray analysis. The major structural characteristic, namely, the sequence of Ti–O distances [1.699(7), 2.006(7), 1.810(2) Å for the centrosymmetric fragment], is in agreement with the bonding scheme shown in Scheme 4. The rather long Ti–THF bond *trans* to the Ti=O bond accounts for the ease with which THF is removed in boiling DME to give **8**.

Although it was not easy to find the appropriate $NaBPh_4$/Ti ratio, the best results were obtained with a 1:1 molar ratio. Changes in the stoichiometry did not affect the ratio between **6** and **7** or result in products other than **6** and **7**. We should emphasize the major difference between the ionization of the Ti–Cl bond with $AgNO_3$ and $NaBPh_4$: the former is fast for both chlorides of **3**, while the latter occurs in a slow stepwise process.

With salen as a ligand, though the reaction with $NaBPh_4$ probably follows the same pathway as for **3**, differences in solubilities allowed different compounds to be isolated

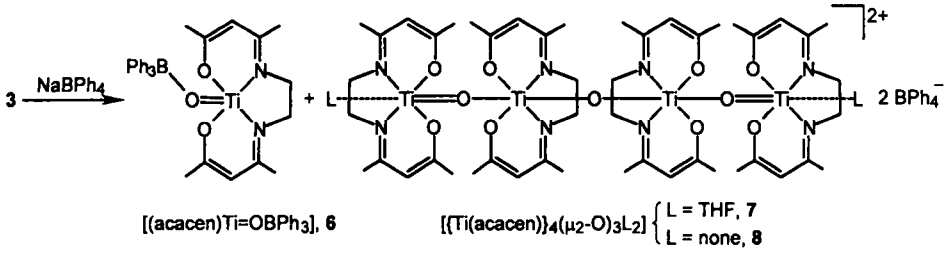

Scheme 4. Reaction of **3** with ionizing agent $NaBPh_4$.

0947-6539/96/0211-1468 $ 15.00+.25/0 Chem. Eur. J. 1996, 2, No. 11

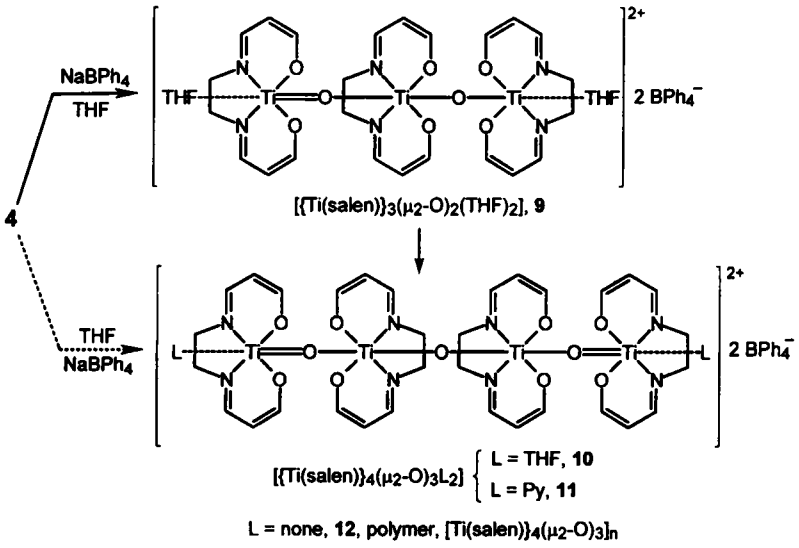

Scheme 5. Ionization of salen complex **4**.

in the solid state. The ionization of **4** led to **10** as the major product (Scheme 5), an analogue of **7**, regardless of the $NaBPh_4$/Ti molar ratio and irrespective of whether the reaction was carried out in THF/H_2O or in THF. It was also possible to identify a second species **9** in the solid crystalline mixture, formed in small but not negligible amounts. This compound is orange.

The structure of **9** consists of packed trimeric cations (Fig. 3), BPh_4^- anions, and disordered THF molecules of crystallization in the molar ratio of 1/2/6. The Ti1-O7-Ti2-O8-Ti3 system is almost linear and has a sequence of Ti–O bond lengths (Table 4) in agreement with the bonding scheme reported in Scheme 5.

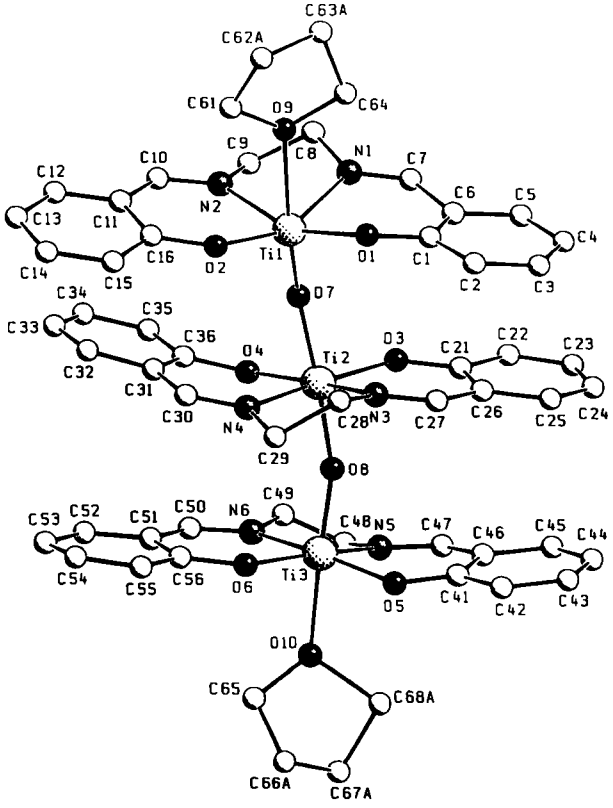

Fig. 3. SCHAKAL drawing of the dication in complex **9**. Disorder involving the THF molecules omitted for clarity.

The structure can be described as a $[Ti\text{-}O\text{-}Ti]^{2+}$ cation solvated by THF and Ti=O. The two THF molecules are at different distances from titanium; the THF *trans* to Ti=O is significantly further away from the metal [Ti1–O9 2.362(7) Å vs. Ti3–O10 2.172(9) Å]. The three independent N_2O_2 cores are planar, in agreement with the hexacoordination around the Ti atoms. The titanium atoms are displaced to differing extents depending on the $Ti-O_{oxo}$ interaction mode; the larger displacement [0.316(1) Å] is observed for Ti1 in the direction of the O7 oxygen atom (Table 5). The structural parameters listed in Table 5 indicate that the six-membered chelation rings are not planar, except for the N2···O2 six-membered chelation rings. The salen ligands[15] assume a "stacked" conformation, with dihedral angles between the N,C_7,O moieties around Ti1, Ti2, and Ti3 of 3.3(2), 10.1(2), and 10.3(3)°, respectively. They are positioned in a columnar stack, in a staggered arrangement with nearly overlapping termi-

Table 4. Selected bond lengths (Å) and angles (°) for complex **9**.

Ti1–O7	1.663(7)	Ti2–O7	1.974(7)	Ti3–O8	1.786(9)
		Ti2–O8	1.846(9)		
Ti1–O1	1.906(7)	Ti2–O3	1.843(7)	Ti3–O5	1.866(7)
Ti1–O2	1.866(7)	Ti2–O4	1.850(7)	Ti3–O6	1.857(7)
Ti1–N1	2.157(8)	Ti2–N3	2.166(7)	Ti3–N5	2.108(10)
Ti1–N2	2.135(7)	Ti2–N4	2.153(10)	Ti3–N6	2.134(10)
Ti1–O9	2.362(7)		Ti3–O10	2.172(9)	
Ti1-O7-Ti2	167.9(4)	O7-Ti2-O8	167.2(3)	Ti2-O8-Ti3	163.2(4)
N1-Ti1-N2	75.6(3)	N3-Ti2-N4	75.9(3)	N5-Ti3-N6	76.3(4)
O2-Ti1-N2	83.9(3)	O4-Ti2-N4	86.0(4)	O6-Ti3-N6	84.9(3)
O2-Ti1-N1	154.1(3)	O4-Ti2-N3	161.3(4)	O6-Ti3-N5	159.5(4)
O1-Ti1-N2	155.3(3)	O3-Ti2-N4	161.2(3)	O5-Ti3-N6	161.4(3)
O1-Ti1-N1	84.7(3)	O3-Ti2-N3	85.4(3)	O5-Ti3-N5	86.9(3)
O1-Ti1-O2	109.8(3)	O3-Ti2-O4	112.3(3)	O5-Ti3-O6	110.3(3)
O7-Ti1-O9	173.4(3)			O8-Ti3-O10	172.8(3)

Table 5. Structural parameters within the Ti(salen) units for complex **9**.

Dist. from N_2O_2 cores, Å					
O1	0.006(9)	O3	0.014(9)	O5	0.001(9)
O2	−0.006(9)	O4	−0.014(9)	O6	−0.001(9)
N1	−0.007(9)	N3	−0.016(9)	N5	−0.001(11)
N2	0.007(9)	N4	0.016(9)	N6	0.002(11)
Ti1	0.316(1)	Ti2	0.074(3)	Ti3	0.161(2)
Folding along/° [a]					
N1···O1	25.6(4)	N4···O4	16.7(4)		
N2···O2	0.2(4)	N5···O5	18.6(4)		
N3···O3	15.0(3)	N6···O6	4.2(4)		
Angles between planes, °					
Ti1-N1-O1/Ti1-N2-O2	24.5(4)	mean $O1\text{-}C_3\text{-}N1/O2\text{-}C_3\text{-}N2$	2.0(4)		
Ti2-N3-O3/Ti2-N4-O4	5.9(4)	mean $O3\text{-}C_3\text{-}N3/O4\text{-}C_3\text{-}N4$	7.6(4)		
Ti3-N5-O5/Ti3-N6-O6	12.7(4)	mean $O5\text{-}C_3\text{-}N5/O6\text{-}C_3\text{-}N6$	10.1(4)		
Torsion angles, °					
N1-C-C-N2	45.8(12)	N3-C-C-N4	−46.8(10)	N5-C-C-N6	−35(2)
Dist. from Ti1-N1-N2 plane, Å					
C8	0.089(13)	C9	−0.531(11)		
Dist. from Ti2-N3-N4 plane, Å					
C28	−0.239(11)	C29	0.408(11)		
Dist. from Ti3-N4-N5 plane, Å					
C48	−0.21(2)	C49	0.21(2)		

[a] The folding is defined as the dihedral angle between the Ti,N,O and OC_3N planes of a six-membered chelation ring.

nal aromatic rings. The dihedral angles between adjacent moieties are: O2,C_7,N2/O4,C_7,N4 14.5(3)°; O4,C_7,N4/O6,C_7,N6 9.8(3); O1,C_7,N1/O3,C_7,N3 9.8(2)°; O3,C_7,N3/O5,C_7,N5 9.4(2)°. The five-membered chelation rings assume a λ conformation for the salen ligands around Ti2 and Ti3 and a δ conformation for the salen ligand around Ti1 (with reference to the coordinates of Table S4, Supplementary Material). Since the space group is chiral, the λ,δ,δ conformer is not present in this structure.

Samples of **9** that were left in the presence of the mother liquor for extended periods converted into red crystals of **10**. The two terminal THF molecules in the tetramer can be replaced by stronger donating solvents, such as pyridine in **11**. The treatment of **10**, however, with weakly binding solvents, such as acetone, led to the polymerization of the tetramer through the sharing of an oxygen from an adjacent tetramer, as shown for **12**. The most significant spectroscopic information on **5**–**12** in the solid state comes from the strong stretching vibrations in the 800–850 cm^{-1} region, associated with the Ti–O bonds. The structures of the related compounds **10** and **12** are shown in Figures 4 and 5.

The structure of **10** consists of centrosymmetric, tetrameric cations and BPh_4^- anions in a molar ratio of 1:2. The tetramer (Fig. 4) contains an approximately linear Ti1–O5–Ti2–O6–Ti2′–O5′–Ti1′ system secured by three oxo oxygen atoms; the central one (O6) is situated on a crystallographic center of symmetry. The pattern of bond lengths and angles in **10** (Table 6) supports the bonding scheme proposed for the tetrameric Ti–O skeleton. The $[Ti\text{-}O\text{-}Ti]^+$ cation is solvated by two titanyl units.

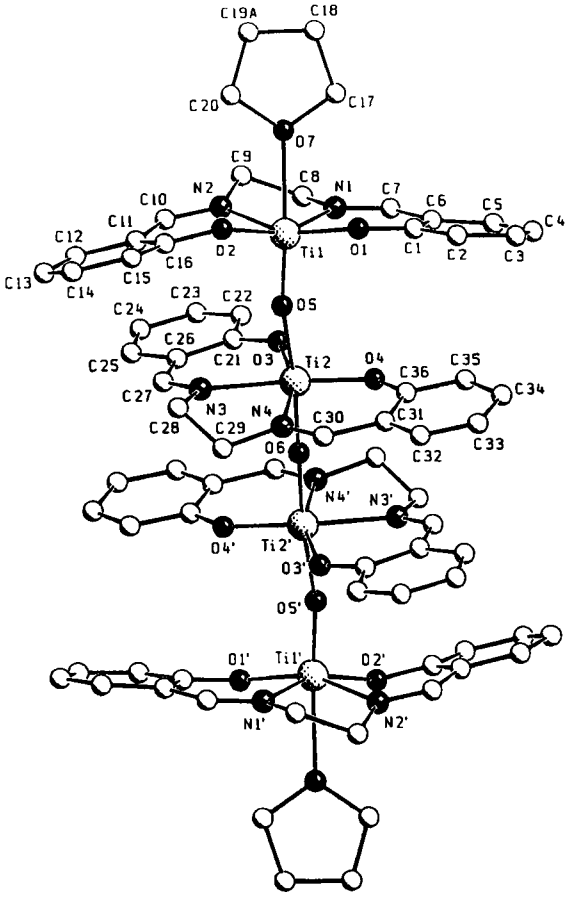

Fig. 4. SCHAKAL drawing of the dication in complex **10**. Disorder involving the THF molecules omitted for clarity. Prime denotes a transformation of $1-x, -y, 1-z$.

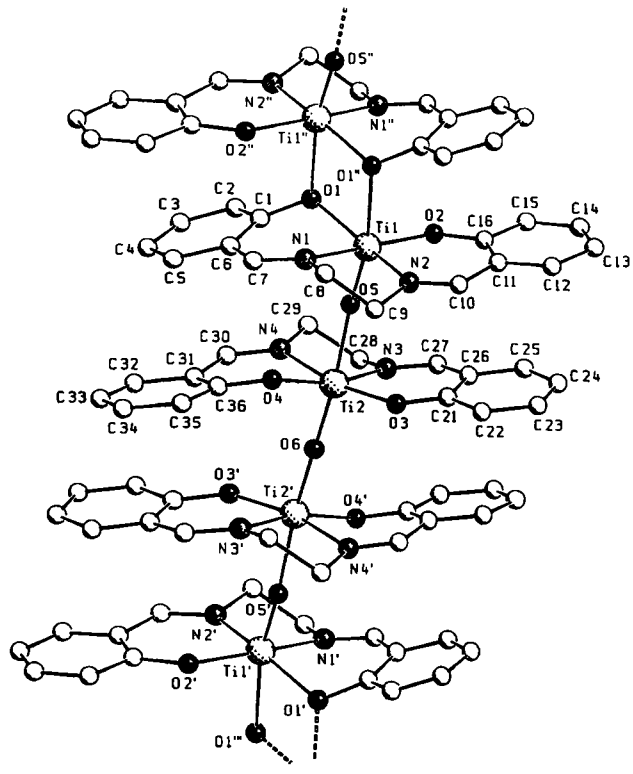

Fig. 5. SCHAKAL drawing of complex **12** showing the chain of cations running along the [100] axis. Prime, double prime, and triple prime denote transformations of $1-x, -y, -z$; $-x, -y, -z$; and $1-x, y, z$, respectively.

Table 6. Selected bond lengths (Å) and angles (°) for complexes **10** and **12** (X represents O7 and O1" for **10** and **12**, respectively).

	10	**12**		**10**	**12**
Ti1–O5	1.714(7)	1.677(5)	Ti1–N1	2.135(9)	2.157(7)
Ti2–O5	2.036(7)	2.040(5)	Ti1–N2	2.140(10)	2.146(7)
Ti2–O6	1.822(2)	1.817(2)	Ti2–O3	1.873(7)	1.867(5)
Ti1–O1	1.893(7)	1.967(5)	Ti2–O4	1.860(7)	1.876(5)
Ti1–O2	1.897(6)	1.865(5)	Ti2–N3	2.160(9)	2.143(6)
Ti1–X	2.373(7)	2.291(6)	Ti2–N4	2.154(9)	2.143(7)
Ti1-O5-Ti2	159.7(4)	163.0(3)	O5-Ti1-X	173.1(3)	168.0(3)
Ti2-O6-Ti2′	180	180	N3-Ti2-N4	75.5(3)	75.7(3)
Ti1-O1-Ti1"		106.0(2)	O4-Ti2-N4	86.1(3)	86.3(2)
N1-Ti1-N2	74.7(4)	75.3(3)	O4-Ti2-N3	160.4(3)	160.9(3)
O2-Ti1-N2	84.8(3)	85.1(2)	O3-Ti2-N4	160.7(3)	160.7(3)
O2-Ti1-N1	155.1(3)	157.5(3)	O3-Ti2-N3	85.3(3)	85.8(2)
O1-Ti1-N2	154.9(4)	153.3(3)	O3-Ti2-O4	112.9(3)	111.4(2)
O1-Ti1-N1	85.3(3)	83.2(3)	O5-Ti2-O6	172.2(2)	167.8(2)
O1-Ti1-O2	109.6(3)	111.9(2)			

The $Ti\text{-}O_{THF}$ bond length [Ti1–O7 2.373(7) Å] *trans* to the Ti1=O5 double bond is quite close to the Ti–O9 bond length in **9**. The geometry of the central dimeric unit (Table 2) is close to that found in complex **5** as far as distances, angles, and relative orientation of the Schiff bases are concerned. The Ti2 atom is displaced by 0.081(2) Å from the N3,O3,N4,O4 core. The N3···N4 five-membered chelation ring assumes a δ conformation. The Ti1 atom is displaced by 0.302(2) Å from the N1,O1,N2,O2 core towards the O5 oxo oxygen. The salen ligand bound to Ti1 assumes a flattened umbrella conformation;[15] the dihedral angle between the two terminal N,C_7,O moieties is 17.3(2)°. The N1···N2 five-membered chelation ring assumes a λ conformation, so that the conformation of the tetramer is $\lambda,\delta,\delta,\lambda$. The behavior of these oligomers was also

0947-6539/96/0211-1470 $ 15.00+.25/0 Chem. Eur. J. 1996, 2, No. 11

investigated in solution by means of variable-temperature ^{1}H NMR spectroscopy. As expected, the spectra are identical for **10** and **12** when they are dissolved in coordinating solvents, such as DMSO. A number of common features are seen for **7** and **12**. For example, coalescence of the CH, CH_2, and CH_3 proton signals is observed. This is also true for the CH and CH_2 proton signals of **12**. We attribute this to an inter-unit exchange process in which a terminal unit dissociates, and a second unit is attached at the other end.

The transformation of **10** to **12** implies the replacement of the terminal THF molecules by the O1 oxygens from the Schiff bases of adjacent tetrameric units[15b] (Fig. 5). This gives rise to zig-zag polymeric chains running along the [100] direction. Bond lengths and angles along the Ti1-O5-Ti2-O6-Ti2′-O5′-Ti1′ system are quite close to those in **10** (Table 6). The value of the Ti1–O1″ bond length [2.291(6) Å] reflects the *trans* influence of the Ti1=O5 double bond. Coordination around each titanium is pseudo-octahedral with the metals significantly displaced from the N_2O_2 cores, by 0.280(2) towards O5 and by 0.118(2) Å towards O6 for Ti1 and Ti2, respectively. The most significant differences between complexes **10** and **12** concern the structural parameters involved in the salen bridging; in particular, a lengthening of the Ti–O1 bond length (Table 6) and a larger folding of the N1···O1 six-membered chelation ring (Table 2). With reference to the coordinates given in Table S6 (Supplementary Material), the five-membered chelation rings assume a δ and λ conformation around Ti1 and Ti2, respectively. The Schiff bases in the tetramer are oriented in such a way that the terminal aromatic rings nearly overlap with the adjacent ethylene bridges; the dihedral angles are O1,C_7,N1/O4,C_7,N4 14.2(1)° and O2,C_7,N2/O3,C_7,N3 6.0(2)°.

b) Theoretical Calculations on μ-Oxo Titanium(IV) Derivatives: Ab initio calculations were performed on the following dinuclear and mononuclear model compounds, where the Schiff base ligand was simulated by two hydroxyl and two ammonia ligands, and the additional O-donor ligands by H_2O: $[\{Cl(OH)_2(NH_3)_2Ti\}_2(\mu_2\text{-}O)]$ (**13**), $[Cl(OH)_2(NH_3)_2Ti(\mu_2\text{-}O)Ti(NH_3)_2(OH)_2]^+$ (**14**), $[\{(OH)_2(NH_3)_2Ti\}(\mu_2\text{-}O)]^{2+}$ (**15**), $[Cl(OH)_2(NH_3)_2Ti(\mu_2\text{-}O)Ti(NH_3)_2(OH)_2(H_2O)]^+$ (**16**), $[\{(H_2O)(OH)_2(NH_3)_2Ti\}_2(\mu_2\text{-}O)]^{2+}$ (**17**), $[Cl(OH)_2(NH_3)_2Ti]^+$ (**18**), and $[(OH)_2(NH_3)_2Ti]^{2+}$ (**19**). Model compounds **13**–**17** are very close to the observed or postulated dinuclear species, while **18** and **19** are the corresponding building blocks.

All the calculations were performed at SCF closed-shell level, because the size of the considered molecules prevents the use of correlated wave-functions. However, the geometries of transition metal complexes in high oxidation states are predicted with good accuracy at SCF level with valence-shell basis sets of double-ζ quality.[16]

Calculations were performed on all complexes in their lowest singlet states. SCF geometry optimization of the geometrical parameters pertaining to the titoxane moiety and Ti–Cl distance led to the values reported in Table 7. The calculated geometries for complexes **13**–**17** can be used to discuss the changes in the nature of the Ti-O-Ti unit upon ionization.

For complex **13**, which is a model of **3**,[8] the results for the optimized parameters show that bond lengths predicted at the HF level are in satisfactory agreement with the experimentally available ones.[8] The Ti–O and the Ti–Cl bond lengths are overestimated by 0.04 and 0.03 Å, respectively. In particular the Ti–O bond length of 1.86 Å confirms that it has weak π character. A less satisfactory agreement is found for the Ti-O-Ti angle, which is calculated to be 155°, while the Ti-O-Ti unit is experimetally found to be linear in complex **3**. However, we observed that the potential surface for **13** varies slowly along the Ti-O-Ti coordinate, so that the linear arrangement in this complex **3** could be due to steric hindrance between the acacen planes and to solid-state packing effects, which are not accounted for in our calculations. It is also worth noting that the value is very close to those observed for analogous complexes with a Ti-O-Ti unit.[7]

Table 7. Optimized geometries (Å and °) for species **13**–**17** and experimental geometries for compounds **3**, **5**, and **7**.

	d(Ti–O)	*d*(Ti′–O)	*d*(Ti–Cl)	∢Ti-O-Ti′
13	1.86	1.86	2.48	155
14	1.98	1.75	2.39	150
15	1.84	1.84	–	153
16	1.95	1.77	2.391	150
17	1.86	1.86	–	153
3	1.86	1.86	–	180
5	1.81	1.81	–	169
7	2.05	1.67	–	163

The results of the geometrical optimization for complexes **14** clearly show that this molecule is based on a titanyl unit. Indeed, from Table 7 we see that the Ti–O bond lengths for ionized and non-ionized titanium are 1.75 and 1.98 Å, respectively. This indicates that the bridging oxygen forms a multiple bond with the titanium that has lost Cl^- and a single bond with the titanium still attached to Cl^-. At the same time there is a substantial *trans* effect of the weakened Ti–O bond on the Ti–Cl bond length; the axial Ti–Cl bond is calculated to be significantly shorter in this species than in the dichloro complex **13** (2.39 vs. 2.48 Å). This indicates a more pronounced π donation from Cl^- to titanium. These Ti–O bond lengths are not too far from those observed for **7**, **9**, **10**, and **12**, which present alternating single and double Ti–O bonds.

The Ti–O bond length obtained from the optimization of the doubly ionized complex **15** (1.84 Å) is very close to that obtained for the non-ionized complex **13** (1.86 Å). This is in agreement with the experimentally reported distances for complex **5** and shows that double ionization does not change the nature of the dimeric $[Ti\text{-}O\text{-}Ti]^{6+}$ unit.

In order to more realistically simulate the solvated species actually found in solution, we repeated the calculations on the singly and doubly ionized model complexes **16** and **17**, with one water molecule coordinated to the ionized titanium. The results give an ionic water–titanium bond, with a fairly long Ti–O distance of about 2.20 Å, and do not show any significant difference in the geometrical parameters pertaining to the Ti-O-Ti moiety compared to the corresponding values for the unsolvated complexes **14** and **15** (Table 7).

The results obtained for complexes **14** and **15**, or for the corresponding solvated **16** and **17**, also indicate that the key step for the formation of the titanyl moiety in the dimeric species is the charge polarization due to the asymmetric single ionization, rather than the ionization itself. The double ionization, in fact, does not lead to any relevant shortening of the Ti–O distance.

Discussion

a) Formation and Properties of Titanoxanes: The self-aggregation of the [Ti–O] functionality in oligomeric forms is the consequence of the induced ionization of the linear [Cl-Ti-O-Ti-Cl] skeleton imposed by the rigid square-planar coordination of the tetradentate Schiff base. In such a colinear skeleton, the donor atoms (the two terminal chlorides and the bridging oxo ligand)

are good σ and π donors. The Ti-O-Ti angle and the Ti–O distances in **3** and **4** support the existence of a significant Ti–O double-bond character due to the oxygen π donation. In the linear skeleton, however, this Ti–O π interaction is in competition with the Ti–Cl π interaction. Replacing the two terminal chlorides with purely non-π-competitive σ donors (see complex **5**) does not affect the Ti-O-Ti moiety, except for some shortening of the Ti-O-Ti bond lengths in the $[O_2NO\text{-}Ti\text{-}O\text{-}Ti\text{-}ONO_2]$ skeleton. Replacing the two terminal chlorides by neutral σ-donor solvent molecules, to give the dicationic form $[S\text{-}Ti\text{-}O\text{-}Ti\text{-}S]^{2+}$, would have the same effect, as supported by our calculations.

What structure would one expect if the ionization of the first terminal chloride occurred much faster than the second? Although we were unable to isolate the hypothetical monocation $[Cl\text{-}Ti\text{-}O\text{-}Ti]^+$, we expect that one of the Ti–O bonds in the resulting nonsymmetric linear skeleton would be strengthened and the other weakened with concomitant shortening of the Ti–Cl bond. Thus the bonding scheme could be rather naively depicted as $[Cl\cdots Ti\text{-}O{=}Ti]^+$. An important corroboration of the bonding schemes in the dimers outlined above comes from the theoretical calculations (vide infra), while some experimental evidence is based on the isolation of **6**–**12**, which contain the Ti=O unit.

We shall now examine the major factors that affect the isolation of the final compound and the identification of the various intermediates. The structure of the Schiff base ligand mainly affects the solubility, which is much higher for acacen than for salen. Another important factor is the kinetic lability of the solvation sphere of titanium(IV), and the pronounced basic properties of the ketone-like Ti=O moiety.[6] Finally, the rate of ionization depends on the ionization agent used (e.g., $AgNO_3$ or $NaBPh_4$). The considerations outlined above led us to suggest Scheme 6 as the general sequence for the rearrangements occurring in the [Cl-Ti-O-Ti-Cl] skeleton upon ionization. We should emphasize that even mild ionization conditions, such as the presence of salts in a solvent or a solvent with a high dielectric constant, can cause the similar rearrangements of the Ti–O bond by ionization of the Ti–Cl bond.

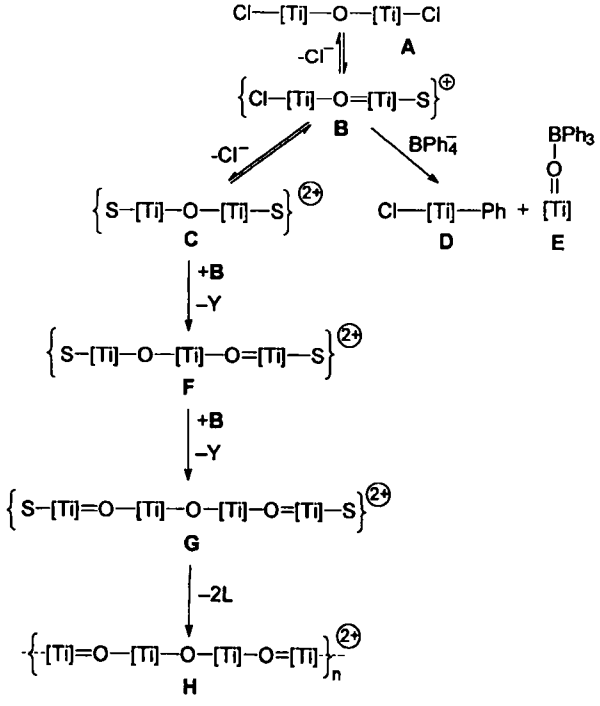

Scheme 6. The stepwise process showing the interconversion of the Ti–O functionalities and their self-assembly. [Ti] = $[Ti(salen)]^{2+}$ or $[Ti(acacen)]^{2+}$; Y = $\{[Ti]\text{-}Cl\}^+$; S = solvent (THF, py, H_2O); counteranion = BPh_4^-.

The compounds given in the results section can be related to those in Scheme 6 as follows: **A**: **3** and **4**; **C**: **5**; **B** and **D**: unidentified; **E**: **6**; **F**: **9**; **G**: **7**, **8**, **10**, **11**; **H**: **12**. Experimental evidence does not exist for **B** as such, though its bonding mode has strong support from the theoretical calculations. The key intermediate in our ionization process is **B**, which makes the [Ti=O] unit available. The titanyl unit plays the role of a competitive solvent towards all the cationic forms. A secondary reaction, namely, the alkylation of **B** by BPh_4^-,[17] generates significant amounts of BPh_3, which partially traps the titanyl unit as the Lewis acid–base adduct **E**. The titanyl unit available from **B** acts as a solvent to form **F**, **G**, and **H**, through a stepwise substitution of the solvent in the dimer **C**. The formation of a solvated or unsolvated form of the tetramer or the appearance of the polymer depends only on the nature of the Schiff base, which is responsible for the differences in solubility, and also on the fact that the solvent molecule *trans* to the Ti=O bond is particularly labile. Indeed, in the structure of **9** there is a significant difference in the two Ti–THF distances; the longer one is *trans* to the Ti=O bond. In this way, the interconversion between solvated, unsolvated, and polymeric forms of the tetrameric skeleton can be explained.

b) Bonding Mode and Molecular Orbital Analysis of μ-Oxotitanium(IV) Dimers: In an effort to understand the factors that determine the interconversion of a bridging into a terminal Ti–O functionality, we performed an analysis of the frontier molecular orbitals and electronic structures of the model complexes **13**–**15** and their building blocks **18** and **19**.

The titanium–oxygen bonding in the dinuclear complexes **13**–**16** may be interpreted in terms of orbital interactions between interacting fragments, namely, an O^{2-} ion and the two species $[(OH)_2(NH_3)_2Ti\text{-}Cl]^+$ or $[(OH)_2(NH_3)_2Ti]^{2+}$. The $[Ti(NH_3)_2(OH)_2]^{2+}$ and $[ClTi(NH_3)_2(OH)_2]^+$ fragments were considered in a pseudo square-planar structure of C_{2v} symmetry and in a pseudo square-pyramidal structure of C_s symmetry, respectively, with the same geometries as those obtained from the optimization of the dinuclear complexes. Their valence MOs are reported in Figures 6 and 7 (left).

The frontier orbitals of $[Ti(NH_3)_2(OH)_2]^{2+}$ in C_{2v} symmetry consists of the five lowest unoccupied orbitals, which are mainly of d character and are ordered as predicted by elementary ligand-field considerations:[18] $14a_1$ (essentially d_{z^2}) is the lowest in energy, and $5b_1$ (d_{xz}) and $3a_2$ (d_{yz}) are slightly higher and almost degenerate, while $11b_2$ (d_{xy}), which points towards the N, O ligands, is by far the highest. When we consider the $[ClTi(NH_3)_2(OH)_2]^+$ complex in C_s symmetry, we find similar frontier orbitals, although we have now three more valence orbitals: the three highest occupied MOs $23a'$, $24a'$, and $14a''$, which essentially describes the Ti–Cl σ bond and two weak Ti-Cl π bonds, respectively.

Figure 6 shows the correlation diagram depicting the MOs for the two $[ClTi(NH_3)_2(OH)_2]^+$ fragments interacting with the MOs of the bridging O^{2-} ligand and reproduces the energy levels of the $[\{Cl(OH)_2(NH_3)_2Ti\}_2(\mu_2\text{-}O)]$ complex that are most relevant to titanium–oxygen bonding. The energy levels for the two $[ClTi(NH_3)_2(OH)_2]^+$ fragments in Figure 6 are given for the separation observed in the final complex (ca. 3.6 Å). Due to extremely small interactions between the two fragments, these levels consist of almost degenerate symmetric and antisymmetric combinations of the levels for the single fragment, which, for the sake of simplicity, are not explicitly distin-

0947-6539/96/0211-1472 $ 15.00+.25/0 Chem. Eur. J. 1996, 2, No. 11

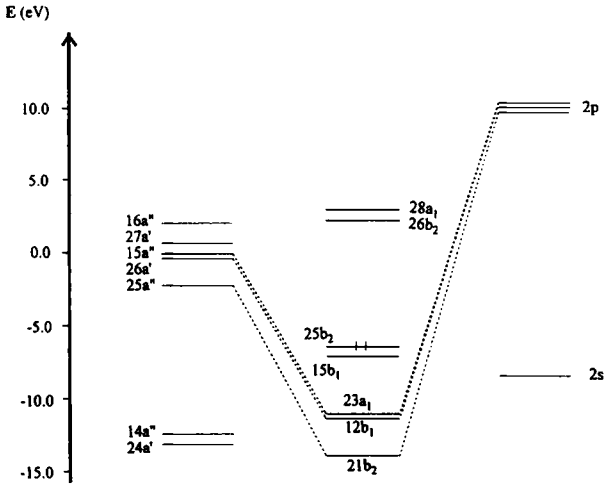

Fig. 6. Molecular orbital correlation diagram for the $[\{Cl(NH_3)_2(OH)_2Ti\}_2(\mu_2\text{-}O)]$ complex in the $^1A_1$ ground state.

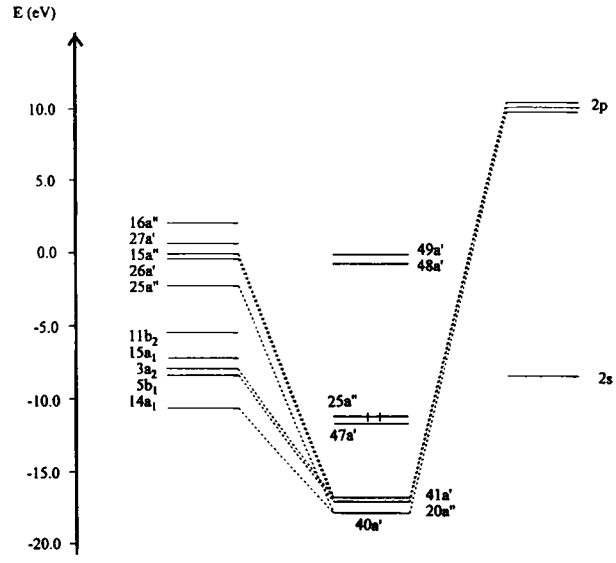

Fig. 7. Molecular orbital correlation diagram for the $[Cl(NH_3)_2(OH)_2Ti(\mu_2\text{-}O)Ti(NH_3)(OH)_2]^+$ complex in the $^1A'$ ground state.

guished. Figure 6 also gives the main valence orbitals of the O^{2-} ion, namely, the doubly occupied 2s orbital and the triply degenerate, fully occupied 2p orbitals. The main bonding orbitals between titanium atoms and the bridging oxygen are: 1) low-lying $21b_2$, which corresponds to a significant overlap between the antisymmetric $3d_{z^2}-3d'_{z^2}$ combination of titanium orbitals and the $2p_z$ orbital of O_2 and therefore describes the Ti–O σ bonds; 2) $12b_1$ and $23a_1$, which correspond to slightly mixed O_2–p_x and p_y orbitals, respectively, with the antisymmetric $3d_{xz}-3d'_{xz}$ and $3d_{yz}-3d'_{yz}$ combinations of titanium orbitals, and therefore describe two Ti–O π bonds. However, owing to the low d_π character of these two MOs, the corresponding π contributions to the Ti–O bond are weak and strongly polarized towards the oxygen. These orbital interactions are illustrated in Scheme 7. The result then is a single σ bond between the titanium and the bridging oxygen, with two weak π-bond contributions. These results reflect the difficulty the titanium triad has forming terminal oxo structures: the high-energy metal orbitals tend to form weak π bonds with oxygen of strongly polarized character; the resulting high charge left on the oxygen then determines the high tendency to bridge.

Scheme 7. One of the two perpendicular three-center MOs involved in Ti–O π bonding in complexes **13** and **15**.

Analogous considerations can be made for the $[\{(OH)_2(NH_3)_2Ti\}_2(\mu_2\text{-}O)]^{2+}$ complex on the basis of the correlation diagram of its MOs in terms of those for the two $[Ti(NH_3)_2(OH)_2]^{2+}$ fragments and the bridging O^{2-} ion. In particular, there is still a low d_π character of the two MOs involved in the Ti–O π bonds, so that the same conclusions can be drawn on the nature of the Ti–O bonds.

A different situation is found when we consider the $[Cl(OH)_2(NH_3)_2Ti(\mu_2\text{-}O)Ti(NH_3)_2(OH)_2]^+$ complex. The correlation diagram of its MOs with those for the two $[Ti(NH_3)_2(OH)_2]^{2+}$ fragments and the bridging O^{2-} ion is shown in Figure 7. Note that now we have two different metal fragments, $[Ti(NH_3)_2(OH)_2]^{2+}$ and $[ClTi(NH_3)_2(OH)_2]^+$; the fragment orbital scheme reported on the left in Figure 7 is slightly more complicated. The energy levels for the two equidistant fragments observed in the final complex consist essentially of those for the two separate fragments. There are three main bonding orbitals between titanium atoms and the bridging oxygen, analogous to those observed for complex **13**: 1) low-lying $40a'$, which corresponds to an almost equivalent overlap between the antisymmetric $c\,3d_{z^2}-c'\,3d'_{z^2}$ combination of titanium orbitals and the $2p_z$ orbital of O_2 (the coefficients c and c' are almost equal so that this orbital describes two essentially equivalent Ti–O σ bonds); 2) $20a''$ and $41a'$, which correspond to O^{2-} p_x and p_y mixed orbitals, respectively, with the antisymmetric $c\,3d_{xz}-c'\,3d'_{xz}$ and $c\,3d_{yz}-c'\,3d'_{yz}$ combinations of titanium orbitals. In this case, however, the metal contribution is significant, but strongly polarized with the c' component of the ionized titanium much higher than the c component of the non-ionized titanium. These two orbitals therefore describe a significant Ti–O π-bond character between the oxygen and the ionized titanium. These two interactions are illustrated in Scheme 8. Thus, we can conclude that the bridging oxygen forms an essentially single σ bond with the non-ionized titanium and a bond with significant multiple-bond character—consisting of two equivalent π_x and π_y contributions—with the ionized titanium.

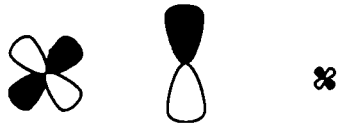

Scheme 8. One of the two perpendicular three-center MOs involved in Ti–O π bonding in complex **14**.

A Mulliken population analysis helps to understand the bonding picture for complexes **13**–**15**. Table 8 lists the Mulliken atomic charges and a few selected populations for complexes

Table 8. Mulliken charges and selected populations for complexes **13**–**15**.

	13	**14**	**15**
Ti	+2.33	+2.26	+2.43
Ti s	6.07	6.13	5.95
Ti d_π	0.39	0.41	0.40
Ti′	+2.33	+2.36	+2.43
Ti′ s	6.07	5.95	5.95
Ti′ d_π	0.39	0.41	0.40
O	−1.20	−1.11	−1.08
O p_π	3.59	3.49	3.61
Cl	−0.54	−0.39	–

13–15. We see that the ionization of one of the two titaniums of complex **13** leaves the charge on it almost unchanged, while there is a reduction of the charge on oxygen. This reflects the increased donation from the bridging oxygen to the ionized titanium, which leads to the larger π-bond character. It is also worth noting that, although the charge on the ionized titanium remains essentially unchanged, there is an internal redistribution with a decrease in the s population and an increase in the d population. This is a consequence of the σ electron density lost with Cl^- in the ionization and d_π density gained by the occupied p_π oxygen orbitals.

Because of the reduced donation from the oxygen, we would expect a charge depletion on the non-ionized titanium. This is not seen, reflecting the increased donation from the terminal chloride, which shows a charge depletion. The effect of the single ionization of **13** can therefore be described as a shift in electron charge from the remaining chlorine atom to the Ti(ionized)–O bond, which leads to the strenghtening of the Ti(ionized)–O and Ti(non-ionized)–Cl bonds and to the weakening of the Ti(non-ionized)–O bond. This effect can be considered as an electronic interpretation of the push–pull principle and is the key factor that leads to the formation and the labilization of the titanyl moiety.

Conclusions

A push–pull principle has been applied to the synthesis and rearrangement of linear titanoxanes. The experimental and theoretical data are in excellent agreement. A push–pull mechanism is observed in the linear Cl-Ti-O-Ti-Cl skeleton, which tries to achieve hexacoordination of the metal ions when one of the two Ti–Cl bonds is ionized. The oxo and chloride ligands are in competition for π donation to the metal; thus, removal of one Cl^- results in a novel Ti–O bonding mode in the $[Cl-Ti-O=Ti]^+$ cation. The [Ti=O] unit becomes very labile and can be used as a building block for the construction of oligomeric and polymeric titanoxanes. This is a novel methodology for producing the fairly reactive [Ti=O] unit, which is hardly accessible through conventional synthetic methods.

Experimental Section

General Procedure: All reactions were carried out under an atmosphere of purified nitrogen. Solvents were dried and distilled before use by standard methods. Infrared spectra were recorded with a Perkin-Elmer FT1600 spectrophotometer. ^{1}H NMR spectra were measured on 200-AC and 400-DPX Bruker instruments. The starting materials **1** [8] and **2** [9] were synthesized according to the reported procedure, while the synthesis of **3** [8] was slightly modified.

Preparation of 3: A deep blue THF (1 L) solution of **1** (56.0 g, 150 mmol) was exposed overnight to dry oxygen to give a red suspension. The mixture was then evaporated to dryness, and toluene (450 mL) added. The resulting suspension was refluxed for 2 h and cooled to room temperature. The red solid collected by filtration (44.2 g, 94%). **3**, $C_{24}H_{36}Cl_2N_4O_5Ti_2$ (627.24): calcd C, 45.90; H, 5.75; N, 8.95; found: C, 45.82; H, 5.71; N, 8.15; ^{1}H NMR (200 MHz, CD_2Cl_2, 298 K): δ = 5.18 (s, 4H, CH), 3.71 (m, 8H, CH_2), 2.04 (s, 12H, CH_3), 1.89 (s, 12H, CH_3); IR (Nujol): $\tilde{\nu}$ = 743 cm^{-1} (Ti–O).

Preparation of 4: A deep green THF (500 mL) solution of **2** (15.0 g, 34.9 mmol) was exposed overnight to dry oxygen. The resulting suspension was concentrated to ca. half its volume, and the orange solid collected by filtration (11.9 g, 87%). **4**·THF, $C_{36}H_{36}Cl_2N_4O_6Ti_2$ (787.37): calcd C, 54.92; H, 4.61; N, 7.12; found: C, 54.25; H, 4.72; N, 6.98; ^{1}H NMR (200 MHz, [D$_6$]acetone, 298 K): δ = 8.92 (s, 4H, CH), 7.93–7.63 (m, 16H, Ph), 4.44 (s, 8H, CH_2), 3.85–3.70 (m, 4H, THF), 2.00–1.90 (m, 4H, THF).

Preparation of 5: $AgNO_3$ (1.10 g, 6.50 mmol) was added in one portion to a red THF (150 mL) suspension of **3** (2.04 g, 3.25 mmol). The flask was immediately covered with aluminum foil, stirred at room temperature for 12 h, and then refluxed overnight. The resulting suspension was filtered, and the brown solid extracted with the mother liquor to remove AgCl. This extract was concentrated to a minimum volume, and the precipitate then collected by filtration (1.4 g, 63.5%). **5**, $C_{24}H_{36}N_6O_{11}Ti_2$ (680.34): calcd C, 42.37; H, 5.33; N, 12.35; found: C, 42.73; H, 5.33; N, 11.81. Crystals suitable for X-ray analysis were obtained by extraction with DME. ^{1}H NMR (400 MHz, [D$_6$]DMSO, 298 K): δ = 5.45 (s, 4H, CH), 3.70–3.60 (m, 8H, CH_2), 2.13 (s, 6H, CH_3), 1.91 (s, 6H, CH_3).

Preparation of 6 and 7: $NaBPh_4$ (1.84 g, 5.38 mmol) was added in one portion to a red THF (150 mL) suspension of **3** (1.69 g, 2.69 mmol), and the mixture refluxed overnight. The resulting suspension was filtered to give a brown solid, which was then extracted with the mother liquor to remove NaCl. The solvent was evaporated to dryness, the residue treated with Et_2O (100 mL), and the resulting brown solid collected by filtration (1.8 g, 70%).

7, $C_{104}H_{128}B_2N_8O_{13}Ti_4$ (1911.35): calcd C, 65.33; H, 6.75; N, 5.86; found: C, 65.62; H, 6.33; N, 5.20. Crystals of **7** suitable for X-ray analysis were grown in a THF/dioxane mixture. ^{1}H NMR (200 MHz, [D$_6$]acetone, 298 K): δ = 7.55–7.45 (m, 16H, BPh_4), 7.15–7.00 (m, 16H, BPh_4), 6.98–6.88 (m, 8H, BPh_4), 5.51 (s, 4H, CH), 5.44 (s, 4H, CH), 4.20–3.82 (m, 16H, CH_2), 3.80–3.73 (m, 8H, THF), 2.35–2.23 (m, 24H, CH_3), 2.15–2.02 (m, 24H, CH_3), 1.98–1.87 (m, 8H, THF). ^{1}H NMR (200 MHz, [D$_6$]DMSO, 373 K): δ = 7.25–7.18 (m, 16H, BPh_4), 6.95–6.87 (m, 16H, BPh_4), 6.81–6.73 (m, 8H, BPh_4), 5.20 (s, 8H, CH), 3.63 (s, 16H, CH_2), 2.03 (s, 24H, CH_3), 1.87 (s, 24H, CH_3).

6 was obtained as yellow crystals from the Et_2O mother liquor. These were suitable for X-ray analysis. $C_{30}H_{39}BN_2O_3Ti$ (534.34): calcd C, 68.20; H, 6.30; N, 5.30; found: C, 68.57; H, 6.21; N, 5.79. ^{1}H NMR (200 MHz, [D$_6$]acetone, 298 K): δ = 7.71–7.43 (m, 6H, BPh_4), 7.20–6.89 (m, 9H, BPh_4), 5.43 (s, 2H, CH), 3.69–3.45 (m, 4H, CH_2), 2.15 (s, 6H, CH_3), 2.09 (s, 6H, CH_3).

Preparation of 8: A DME (150 mL) suspension of **7** (2.36 g, 1.25 mmol) was refluxed overnight. The brown solid was collected by filtration (0.88 g, 40%). $C_{96}H_{112}B_2N_8O_{11}Ti_4$ (1767.13): calcd C, 65.26; H, 6.39; N, 6.34; found: C, 64.91; H, 6.49; N, 6.14. Crystals suitable for X-ray analysis were obtained by extraction with DME. ^{1}H NMR (200 MHz, [D$_6$]acetone, 298 K): δ = 7.55–7.42 (m, 16H, BPh_4), 7.13–7.01 (m, 16H, BPh_4), 6.95–6.86 (m, 8H, BPh_4), 5.52 (s, 4H, CH), 5.44 (s, 4H, CH), 4.10–3.85 (m, 16H, CH_2), 2.35–2.24 (m, 24H, CH_3), 2.15–2.00 (m, 24H, CH_3).

Preparation of 9 and 10: $NaBPh_4$ (1.10 g, 3.19 mmol) was added in one portion to an orange THF (100 mL) suspension of **4**·THF (1.16 g, 1.47 mmol), and the mixture refluxed overnight. The resulting suspension was filtered, and the solid extracted with the mother liquor to remove NaCl. Filtration of these extracts gave 0.6 g of product. The remaining light-yellow solution was cooled to 4 °C to yield a mixture of red (**10**) and light-orange (**9**) crystals. The orange product was extracted with THF (100 mL) until crystals of **10** and **9** were obtained. The extraction was then continued with fresh THF (100 mL) to obtain pure crystalline **10**. The final quantities obtained after the extraction were 0.45 g of **9** and 0.15 g of **10**. All the crystals obtained were suitable for X-ray analysis.

10, $C_{120}H_{112}B_2N_8O_{13}Ti_4$ (2087.40): calcd C, 69.05; H, 5.41; N, 5.37; found: C, 68.00; H, 5.11; N, 5.18. ^{1}H NMR (400 MHz, [D$_6$]DMSO, 298 K): δ = 8.16 (s, 2H, CH), 8.01 (s, 2H, CH), 8.60 (s, 2H, CH), 7.39 (s, 2H, CH), 7.27–7.17 (m, 26H, 10 Ph + 16 BPh_4), 7.15–7.05 (m, 8H, Ph), 6.95–6.88 (m, 16H, BPh_4), 6.82–6.77 (m, 8H, BPh_4), 6.73–6.10 (m, 14H, Ph), 3.80–3.68 (m, 16H, 8CH_2 + 8THF), 3.64–3.50 (m, 8H, CH_2), 1.78–1.70 (m, 8H, THF).

9, $C_{104}H_{98}B_2N_6O_{10}Ti_3$ (1757.22): C, 71.09; H, 5.62; N, 4.78; found: C, 69.96; H, 5.89; N, 4.50. ^{1}H NMR (200 MHz, [D$_6$]DMSO, 298 K): δ = 8.13 (s, 4H, CH), 7.58 (s, 2H, CH), 7.50–7.05 (m, 24H, 8Ph + 16BPh_4), 6.95–6.88 (m, 16H, BPh_4), 6.81–6.21 (m, 24H, 16 Ph + 8 BPh_4), 3.96–3.90 (m, 4H, CH_2), 3.85–3.65 (m, 8H, CH_2), 3.62–3.50 (m, 8H, THF), 1.85–1.70 (m, 8H, THF).

Preparation of 11: A pyridine suspension of **12** (1.33 g, 0.682 mmol) was heated until the solid dissolved. The orange solution was concentrated to half its volume, and *n*-hexane (100 mL) was added. The product precipitated (1.1 g, 78%). **11**, $C_{122}H_{106}B_2N_{10}O_{11}Ti_4$ (2101.38): calcd C, 69.73; H, 5.08; N, 6.67; found: C, 70.30; H, 4.74; N, 6.68.

Preparation of 12: $NaBPh_4$ (4.0 g, 11.7 mmol) was added in one portion to a THF (200 mL) suspension of **4**·THF (4.27 g, 5.84 mmol). A red suspension was obtained, which was refluxed for 12 h. The solid was then filtered and extracted with the mother liquor to remove NaCl. The volume of this mixture was reduced to 100 mL, and the resulting red solid collected, dried, and suspended in acetone (200 mL). This suspension was then stirred at room temperature for 5 h and refluxed overnight. The solid was filtered off and the solution evaporated to dryness. The pale red residue was then treated with Et_2O (150 mL) to yield the product (3.8 g, 67%). $C_{112}H_{96}B_2N_8O_{11}Ti_4$ (1943.18): calcd C, 69.29; H, 4.98; N, 5.77; found: C, 70.04; H, 4.97; N, 4.95. Crystals suitable for X-ray analysis were grown in deuterated acetone and contain acetone as solvent of crystallization (Ti:acetone = 2:1). ^{1}H NMR (400 MHz, [D$_6$]DMSO, 298 K): δ = 8.14 (s, 2H, CH), 8.01 (s, 2H, CH), 7.55 (s, 2H, CH), 7.39 (s, 2H, CH), 7.32–7.16 (m, 26H, 10Ph + 16BPh_4), 7.10–7.00 (m, 8H, Ph), 6.94–6.90 (m, 16H, BPh_4), 6.80–6.77 (m, 8H, BPh_4), 6.74–6.08

0947-6539/96/0211-1474 $ 15.00+.25/0 Chem. Eur. J. 1996, 2, No. 11

Table 9. Experimental data for the X-ray diffraction studies on crystalline compounds **5**, **6**, **9**, **10**, and **12**.

	5	**6**	**9**	**10**	**12**
formula	$C_{24}H_{36}N_6O_{11}Ti_2$	$C_{30}H_{33}BN_2O_3Ti \cdot 2C_{24}H_{20}B \cdot 6C_4H_8O$	$C_{56}H_{58}N_6O_{10}Ti_3 \cdot 2C_{24}H_{20}B$	$C_{72}H_{72}N_8O_{13}Ti_4 \cdot 2C_{24}H_{20}B \cdot 2C_3D_6O$	$C_{64}H_{56}N_8O_{11}Ti_4 \cdot$
a (Å)	14.966(5)	11.202(2)	33.031(5)	11.121(2)	13.816(3)
b (Å)	16.158(5)	16.656(2)	15.883(3)	26.549(4)	16.611(6)
c (Å)	12.767(6)	15.687(2)	22.471(4)	17.729(2)	22.262(4)
α, γ (°)	90	90	90	90	90
β (°)	90	102.94(1)	90	96.52(1)	101.47(2)
V (Å^3)	3087(2)	2852.6(7)	11789(4)	5200.7(14)	5007(2)
Z	4	4	4	2	2
M_r	680.4	528.3	2189.9	2087.5	2071.5
space group	$P2_12_12_1$ (no. 19)	$P2_1/c$ (no. 14)	$Pna2_1$ (no. 33)	$P2_1/c$ (no. 14)	$P2_1/n$ (no. 14)
T (°C)	22	22	−138	22	−150
λ (Å)	0.71069	1.54178	1.54178	1.54178	1.54178
ρ_{calcd} (g cm^{-3})	1.464	1.230	1.234	1.333	1.374
μ (cm^{-1})	5.73	27.90	22.03	30.68	31.80
transm. coeff.	0.908–1.000	0.964–1.000	0.781–1.000	0.745–1.000	0.642–1.000
unique total data	5449	5316 (NO)	10595 (NO)	9713 (NO)	9777
criterion for obs.	$I > 2\sigma(I)$	$I > 2\sigma(I)$	$I > 2\sigma(I)$	$I > 2\sigma(I)$	$I > 2\sigma(I)$
unique obs. data	3411 (NO)	1929	5379	2838	4474 (NO)
R [a]	0.044 [0.045]	0.052	0.071 [0.071]	0.079	0.067
$wR2$ [b]	0.115 [0.153]	0.203	0.247 [0.248]	0.234	0.174
GOF [c]	1.034	0.971	1.011	1.068	1.109

[a] Values in square brackets refer to the "inverted structure". $R = \sum|\Delta F|/\sum|F_o|$ calculated for the unique observed reflections. [b] $wR2 = [\sum w|\Delta F^2|^2/\sum w|F_o^2|^2]^{1/2}$ calculated for the unique total data for **6**, **9**, **10** and for the unique observed data for **5**, **12**. [c] GOF $= [\sum w|\Delta F^2|^2/(NO - NV)]^{1/2}$.

(m, 14H, Ph), 3.77–3.72 (m, 8H, CH_2), 3.62–3.56 (m, 8H, CH_2). ^{1}H NMR (200 MHz, [D$_6$]DMSO, 398 K): δ = 7.83 (s, 8H, CH), 7.29–7.16 (m, 28H, 12Ph + 16 BPh$_4$), 6.96–6.88 (m, 24H, 16Ph + 8BPh$_4$), 6.82–6.75 (m, 8H, BPh$_4$), 6.65–6.57 (m, 6H, Ph), 6.37–6.33 (m, 6H, Ph), 3.74 (s, 16H, CH_2).

X-Ray crystallography for complexes 5, 6, 9, 10, and 12. Suitable crystals were mounted in glass capillaries and sealed under nitrogen. The reduced cells were obtained by using TRACER [19]. Crystal data and details associated with data collection are given in Tables 9 and S1 (Supplementary Material). All the data were collected on a Rigaku AFC6S single-crystal diffractometer at 295 K for complexes **5**, **6**, and **10**, and at 135 K for **9**, and at 123 K for **12**. For intensities and background the individual reflection profiles were analyzed [20]. The structure amplitudes were obtained after the usual Lorentz and polarization corrections [21], and the absolute scale was established by the Wilson method [22]. The crystal quality was tested by ψ scans showing that crystal absorption effects could not be neglected. Data were then corrected for absorption using a semiempirical method for all complexes [23]. The function minimized during the least-squares refinement was $\sum w(\Delta F^2)^2$. Anomalous scattering corrections were included in all structure factor calculations [24b]. Scattering factors for neutral atoms were taken from ref. [24a] for non-hydrogen atoms and from ref. [25] for H. Structure solutions were based on the observed reflections [$I > 2\sigma(I)$]. The refinements were carried out with SHELXL 92 [26] with the unique observed reflections for complexes **5** and **12**, and the unique total reflections for complexes **6**, **9**, and **10**.

The structures were solved by the heavy-atom method starting from a three-dimensional Patterson map for **5**, **6**, **9**, and **10** by using SHELX 76 [27] and by direct methods for **12** by using SHELX 86 [28]. Refinements were carried out by full-matrix least-squares first isotropically, then anisotropically for all the non-H atoms, except for the disordered atoms. Some atoms of coordinated THF molecules in complexes **9** and **10** were affected by high thermal parameters indicating the presence of disorder. This was solved by splitting the atoms over two positions (A and B) isotropically refined with site occupation factors of 0.5. In complex **9** the same kind of disorder affected also the six independent THF molecules of crystallization. In complex **12** the acetone solvent molecule of crystallization was found to be affected by disorder. The best fit was obtained by considering the molecule to be statistically distributed over three positions (A, B, and C) isotropically refined with the site occupation factors of 0.85 for C81, C83A, 0.7 for O7A, C82A, 0.3 for C82B, C83B, and 0.15 for O7C, C84B. All hydrogen atoms, except those associated to the disordered carbon atoms, that were ignored, were located from difference Fourier maps and introduced in the subsequent refinements as fixed-atom contributions with isotropic U's fixed at 0.08 for **5**, **6**, **9**, **12** and 0.10 Å^2 for **10**. In the last stage of refinement the weighting scheme $w = 1/[\sigma^2(F_o^2) + (aP)^2]$ (with $P = (F_o^2 + 2F_c^2)/3$ and a = 0.0802, 0.0869, 0.1540, 0.0000, and 0.1010 for **5**, **6**, **9**, **10**, and **12**, respectively) was applied. During the refinement of complex **9** the C–O and C–C bond lengths within the disordered THF molecules were constrained to be 1.48(1) and 1.54(1) Å, respectively. The final difference maps showed no unusual feature, with no significant peak above the general background.

The crystal chirality of complexes **5** and **9**, which crystallize in polar space groups, was tested by inverting all the coordinates (x, y, $z \rightarrow -x$, $-y$, $-z$) and refining to convergence again. The resulting R values quoted in Table 9 in square brackets indicated that the original choice should be considered the correct one.

Final atomic coordinates are listed in the Supplementary Material in Tables S2-S7 for non-H atoms and in Tables S8-S13 for hydrogens. Thermal parameters are given in Tables S14-S19, bond lengths and angles in Tables S20-S25.

Crystallographic data (excluding structure factors) for the structures reported in this paper have been deposited with the Cambridge Crystallographic Data Centre as supplementary publication no. CCDC-1220-32. Copies of the data can be obtained free of charge on application to The Director, CCDC, 12 Union Road, Cambridge CB21EZ, UK (Fax: Int. code +(1223)336-033; e-mail: teched@chemcrys.cam.ac.uk).

Computational Details

a) Basis set: The s,p basis for titanium was taken from the (12s6p4d) set of ref. [29] with the addition of two basis functions to describe the 4p orbital [30] and the deletion of the outermost s function, while the Ti d basis was the reoptimized (5d) set of ref. [31], contracted (4/1). This leads to an (11s8p5d) primitive basis for titanium, contracted (8s6p2d). A split valence expansion was used for all the other ligand atoms, with a (11s7p/6s4p) basis for chlorine [32] and a (9s5p/3s2p) contraction for nitrogen and oxygen [31], while a (3s/1s) minimal basis was used for hydrogen [31].

b) Methods: All the calculations were performed at SCF level. The LCAO-SCF-MO scheme was employed both to derive ground state energies and wave functions for all the investigated structures and to perform the various geometry optimizations and transition state calculations. All computations were performed by using the GAMESS program package [33], implemented on IBM RS 6000 workstations.

c) Geometry and geometry optimization: In the model used for the calculations, the Schiff base ligands were simulated with two OH^- and two NH_3 ligands, with the N_2O_2 core fixed to lie in a plane also containing the titanium atom. In all the complexes the Ti–O or Ti–Cl directions were fixed perpendicular to the N_2O_2 co-ordination plane. We optimized only the geometrical parameters pertaining to the Ti-O-Ti moiety, i.e., Ti–O bond lengths, the Ti-O-Ti angle, and the Ti–Cl bond length. All other parameters were fixed to the experimental values or to values taken from OH^-, NH_3, and H_2O molecules. In the binuclear complexes the coordinate system were chosen so that the z axis was pointed in the Ti–Ti direction. As the optimized Ti-O-Ti angles differs slightly from 180°, the z axis diverges slightly from the Ti–O direction. Owing to the bend in the Ti-O-Ti unit, there is a slight mixing of the d_σ and d_π contributions, which is, however, small and has been neglected in the discussion.

Acknowledgements: This work was supported by the Fonds National Suisse de la Recherche Scientifique (Grant. No. 20-40268.94) and COST (Action D3).

Received: March 27, 1996 [F334]

[1] a) P. A. Cox, *The Electronic Structure and Chemistry of Solids*, Oxford University Press, Oxford, UK, **1987**. b) P. A. Cox, *Transition Metal Oxides, an Introduction to Their Electronic Structure and Properties*, Clarendon, Oxford, UK, **1992**.

[2] a) L. M. Babcock, W. G. Klemperer, *J. Chem. Soc. Chem. Commun.* **1987**, 858. b) L. M. Babcock, W. G. Klemperer, *Inorg. Chem.* **1989**, *28*, 2003. V. W. Day,

T. A. Eberspacher, W. G. Klemperer, C. W. Park, F. S. Rosenberg, *J. Am. Chem. Soc.* **1991**, *113*, 8190. c) V. W. Day, T. A. Eberspacher, W. G. Klemperer, C. W. Park, *ibid.* **1993**, *115*, 8469. d) R. Andrés, M. V. Galakhov, A. Martin, M. Mena, C. Santamaria, *Organometallics* **1994**, *13*, 2159 and references therein. e) A. Roth, C. Floriani, A. Chiesi-Villa, C. Guastini, *J. Am. Chem. Soc.* **1986**, *108*, 6823. f) T. Carofiglio, C. Floriani, M. Rosi, A. Chiesi-Villa, C. Rizzoli, *Inorg. Chem.* **1991**, *30*, 3245. g) T. Carofiglio, C. Floriani, A. Sgamellotti, M. Rosi, A. Chiesi-Villa, C. Rizzoli, *J. Chem. Soc. Dalton Trans.* **1992**, 1081. h) T. Carofiglio, C. Floriani, A. Roth, A. Sgamellotti, M. Rosi, A. Chiesi-Villa, C. Rizzoli, *J. Organometal. Chem.* **1995**, *488*, 141.

[3] A. Roth, C. Floriani, A. Chiesi-Villa, C. Guastini, *J. Am. Chem. Soc.* **1986**, *108*, 6823.

[4] a) V. Day, W. G. Klemperer, *Science* **1985**, *228*, 533. b) F. Bottomley, L. Sutin, *Adv. Organomet. Chem.* **1988**, *28*, 339 and references therein. c) C. F. Campana, Y. Chen, V. W. Day, W. G. Klemperer, R. A. Sparks, *J. Chem. Soc. Dalton Trans.* **1996**, 691.

[5] a) M. M. Olmstead, P. P. Power, M. Viggiano, *J. Am. Chem. Soc.* **1983**, *105*, 2927. b) G. R. Willey, J. Palin, M. G. B. Drew, *J. Chem. Soc. Dalton Trans.* **1994**, 1799. c) K. Wieghardt, U. Quilitzsch, J. Weiss, B. Nuber, *Inorg. Chem.* **1980**, *19*, 2514. d) A. Bodner, P. Jeske, T. Weyhermüller, K. Wieghardt, E. Dubler, H. Schmalle, B. Nuber, *ibid.* **1992**, *31*, 3737.

[6] a) C.-H. Yang, V. L. Goedken, *Inorg. Chim. Acta* **1986**, *117*, L19. b) C.-H. Yang, J. A. Ladd, V. L. Goedken, *J. Coord. Chem.* **1988**, *19*, 235. c) R. Guilard, C. Lecomte, *Coord. Chem. Rev.* **1985**, *65*, 87. d) P. Jeske, G. Haselhorst, T. Weyhermueller, K. Wieghardt, B. Nuber, *Inorg. Chem.* **1994**, *33*, 2462. e) P. Comba, A. Merbach, *Inorg. Chem.* **1987**, *26*, 1315. f) S. De Angelis, E. Solari, C. Floriani, A. Chiesi-Villa, C. Rizzoli, *Organometallics* **1995**, *14*, 4505. g) R. Guilard, J. M. Latour, C. Lecomte, J. C. Marchon, J. Protas, D. Ripoll, *Inorg. Chem.* **1978**, *17*, 1228. h) L. Peng-Ju, H. Sheng-Hua, H. Kun-Yao, W. Ru-Ji, T. C. W. Mak, *Inorg. Chim. Acta* **1990**, *175*, 105. i) M. R. Smith III, P. T. Matsunaga, R. A. Andersen, *J. Am. Chem. Soc.* **1993**, *115*, 7049. D. J. Schwartz, M. R. Smith III, R. A. Andersen, *Organometallics* **1996**, *15*, 1446. j) N. P. Dwyer, L. Puppe, J. W. Buchler, W. R. Scheidt, *Inorg. Chem.* **1975**, *14*, 1782.

[7] C. E. Housmekerides, D. L. Ramage, C. M. Kretz, J. T. Shontz, R. S. Pilato, G. L. Geoffroy, A. L. Rheingold, B. S. Haggerty, *Inorg. Chem.* **1992**, *31*, 4453.

[8] M. Mazzanti, J.-M. Rosset, C. Floriani, A. Chiesi-Villa, C. Rizzoli, *J. Chem. Soc. Dalton Trans.* **1989**, 953.

[9] M. Pasquali, F. Marchetti, A. Landi, C. Floriani, *J. Chem. Soc. Dalton Trans.* **1978**, 545.

[10] J. March, *Advanced Organic Chemistry*, 4th ed., Wiley, New York, **1992**, pp. 55, 129, 190 and references therein.

[11] E. Gallo, E. Solari, F. Franceschi, C. Floriani, A. Chiesi-Villa, C. Rizzoli, *Inorg. Chem.* **1995**, *34*, 2495.

[12] U. Thewalt, H.-P. Klein, *Z. Anorg. Allg. Chem.*, **1981**, *479*, 113.

[13] H.-P. Klein, U. Thewalt, *J. Organometal. Chem.* **1981**, *206*, 69.

[14] a) F. Corazza, E. Solari, C. Floriani, A. Chiesi-Villa, C. Guastini, *J. Chem. Soc. Dalton Trans.* **1990**, 1335. b) E. Solari, F. Corazza, C. Floriani, A. Chiesi-Villa, C. Guastini, *ibid.* **1990**, 1345. c) J.-M. Rosset, C. Floriani, M. Mazzanti, A. Chiesi-Villa, C. Guastini, *Inorg. Chem.* **1990**, *29*, 3991.

[15] a) E. Solari, C. Floriani, A. Chiesi-Villa, C. Rizzoli, *J. Chem. Soc. Dalton Trans.* **1992**, 367. b) M. Calligaris, L. Randaccio, in *Comprehensive Coordination Chemistry, Vol. 2* (Eds.: G. Wilkinson, R. D. Gillard, J. A. McCleverty), Pergamon, Oxford, UK, **1987**, Chapt. 20.1, p. 715. c) G. Dell'Amico, F. Marchetti, C. Floriani, *J. Chem. Soc. Dalton Trans.* **1982**, 2197; d) G. Gilli, D. W. J. Cruickshank, R. C. Beddocs, O. S. Mills, *Acta Crystallogr. Sect. B* **1972**, *B28*, 1889.

[16] A. Neuhaus, A. Veldkamp, G. Frenking, *Inorg. Chem.* **1994**, *33*, 5278.

[17] For BPh_4^- acting as an alkylating agent, see: a) J. M. Forward, J. P. Fackler Jr., R. J. Staples, *Organometallics* **1995**, *14*, 4194. b) A. Sladek, S. Hofreiter, M. Paul, H. Schmidbaur, *J. Organometal. Chem.* **1995**, *501*, 47. c) S. H. Strauss, *Chem. Rev.* **1993**, *93*, 927. d) C. S. Cho, S. Motofusa, K. Ohe, S. Uemura, *J. Org. Chem.* **1995**, *60*, 883. e) I. F. Pickersgill, A. P. Marchington, C. M. Rayner, *J. Chem. Soc. Chem. Commun.* **1994**, 2597.

[18] B. N. Figgis, *Introduction to ligand fields*, Wiley-Interscience, New York, **1966**.

[19] S. L. Lawton, R. A. Jacobson, *TRACER (a cell reduction program)*; Ames Laboratory, Iowa State University of Science and Technology, Ames, IA, **1965**.

[20] M. S. Lehmann, F. K. Larsen, *Acta Crystallogr. Sect. A: Cryst. Phys.. Diffr. Theor. Gen. Crystallogr.* **1974**, *A30*, 580-584.

[21] Data reduction, structure solution, and refinement were carried out on an IBM PS2/80 personal computer and on an ENCORE 91 computer.

[22] A. J. C. Wilson, *Nature* **1942**, *150*, 151.

[23] A. C. T. North, D. C. Phillips, F. S. Mathews, *Acta Crystallogr. Sect. A: Cryst. Phys. Diffr. Theor. Gen. Crystallogr.* **1968**, *A24*, 351.

[24] a) *International Tables for X-ray Crystallography*; Kynoch Press, Birmingham, England, 1974; Vol. IV, p. 99. b) *ibid.*, p. 149.

[25] R. F. Stewart, E. R. Davidson, W. T. Simpson, *J. Chem. Phys.* **1965**, *42*, 3175.

[26] G. M. Sheldrick, *SHELXL92: Program for Crystal Structure Refinement*; University of Göttingen: Göttingen, Germany, **1992**.

[27] G. M. Sheldrick, *SHELX76: Program for Crystal Structure Determination*; University of Cambridge: Cambridge, England, **1976**.

[28] G. M. Sheldrick, *SHELXL86: Program for the Solution of Crystal Structures*; University of Göttingen, Germany, **1986**.

[29] R. Roos, A. Veillard, G. Vinot, *Theor. Chim. Acta* **1971**, *20*, 1.

[30] D. M. Hood, R. M. Pitzer, H. F. Schaeffer III, *J. Chem. Phys.* **1979**, *71*, 705.

[31] Y. Sakai, H. Tatewaki, S. Huzinaga, *J. Comput. Chem.* **1981**, *2*, 100.

[32] T. H. Dunning, Jr., *J. Chem. Phys.* **1970**, *53*, 2823.

[33] M. F. Guest, P. Sherwood, *GAMESS User Manual*, Daresbury Technical Memorandum, Daresbury Laboratory, **1991**.

0947-6539/96/0211-1476 $ 15.00+.25/0